A strain-based criterion for failure load prediction of steel/CFRP double strap joints

S.M.J. Razavi [1,2], M.R. Ayatollahi [2], H.R. Majidi [2], F. Berto [1*]

[1] *Department of Mechanical and Industrial Engineering, Norwegian University of Science and Technology (NTNU), Richard Birkelands vei 2b, 7491 Trondheim, Norway.*

[2] *Fatigue and Fracture Research Laboratory, Center of Excellence in Experimental Solid Mechanics and Dynamics, School of Mechanical Engineering, Iran University of Science and Technology, Narmak, 16846 Tehran, Iran*.

Abstract

One of the most effective approaches to improve the strength of steel structures is using the carbon fiber reinforced polymer (CFRP) as externally-bonded sheets. In this paper, a strain-based failure criterion, namely the critical normal strain (CNS) is employed to predict the failure load of adhesively bonded double strap joints which are made of CFRP and steel plates. According to this approach, the adhesive joint fails when the normal strain along the adhesive mid-line attains a critical value at a critical distance. This work is based on a two-dimensional linear elastic finite element analysis. Failure load capacities are estimated theoretically for steel/CFRP double strap joints with different bonding lengths. The predicted values of failure loads are compared with the experimental data reported in literature. It is shown that a good consistency exists between the experimental failure loads and the theoretical predictions based on the new strain-based criterion.

Keywords:

Adhesive joint; CFRP; Failure load prediction; Double strap joint; Steel structure.

[*] Corresponding author: F. Berto (E-mail: Filippo.berto@ntnu.no)

Nomenclature

B	width of the substrate
CFRP	carbon fibre reinforced polymer
CNS	critical normal strain
CZM	cohesive zone model
DSJ	double strap joint
E_{adh}	tensile modulus of the adhesive layer
E_{CFRP}	tensile modulus of the CFRP sheets
E_{eq}	equivalent modulus of CFRP/adhesive layer
FRP	fibre reinforced polymer
L_1 & L_2	bonding length
L_{cr}	critical distance
L_{sub}	substrate length
t_{adh}	thickness of the adhesive layer
t_{CFRP}	thickness of the CFRP layer
t_{sub}	thickness of the substrate
x	distance from the bonding edge
MHSM	modified Hart smith model
P_{CNS}	theoretical failure load predicted by CNS criterion
$P_{Exp.}$	experimental failure load
SLJ	single lap joint

1. Introduction

Carbon fibre reinforced polymer (CFRP) sheets have many applications in industrial components, for instance they are used in order to increase the service life and load carrying capacities of damaged steel

structures. Nowadays, Due to the reduced weight and cost of CFRP laminates, they are often applied in retrofitting of steel structures instead of utilizing the conventional mechanical fastening procedures like welding or bolting. In huge industries like aerospace, wind energy, marine structures, etc., application of CFRP laminates is widely growing. One of the major applications of CFRP laminates is to reduce the overall weight of structures. For instance, it can be pointed to Boeing 787 aircraft, in which 43% of metal structures including fuselage, wing, etc. were replaced by CFRP laminates. Therefore, since CFRP have attracted considerable attention as a new retrofitting material to increase the LBC and the service life of structural components, proposing a suitable failure prediction model to estimate the load bearing capacities (LBCs) of the steel/CFRP bonded joints can be very necessary.

Up to now, many approaches have been proposed to analyze the behavior of steel components strengthened with CFRP patches [1-5], including nonlinear theory [6], digital image correlation (DIC) [7-10], extended finite element method (XFEM) [11, 12] and cohesive zone model (CZM) [13-16]. Determination of failure mechanisms in steel/CFRP adhesive bonded joints is an important issue due to its undeniable effect on the operational life of the components. Several failure criteria have been proposed by researchers to predict the failure load of adhesively bonded joints. The majority of the available failure criteria are based on stress, strain or energy condition in the bond layer [17-24]. Due to their importance shear stress and normal stress (also known as peel stress) values were considered as the key parameters in failure assessments.

The double strap joints (DSJ) are one of the commonly used test specimens for investigating the adhesion strength between steel plates and composite sheets. DSJs are made of two steel plates and CFRP sheets on each side of the joints, as shown in Fig. 1. The CFRP sheets are bonded to the steel substrates using structural adhesive. Critical energy as a common failure approach was utilized for double strap joints (DSJ) by some researchers [25, 26]. Chalkley and Rose [27] modified the Hashin's variational method and Barroso et al. [28] took into account the stress singularity effects to evaluate

failure in double lap joints. In a similar study, Lee et al. extracted the joint strength and the failure modes of steel/GFRP bonded DSJs experimentally [29].

Numerous researchers investigated the strength of CFRP/steel DSJs experimentally and studied the influence of various parameters on the joint strength (see for instance [30-38]). Zhao et al. studied the bond strength and fatigue crack propagation between steel and FRP sheets in a review article [39]. Another review article published recently by Mohee et al. [40] has explored the strength, design parameters, performance, and failure modes of the CFRP joints. Additionally, Fawzia et al. investigated the bond strength between steel plates and CFRP strips by a series of DSJs tested under axial tensile loading [32]. They used a modified Hart-smith model for predicting the failure load in steel/CFRP DSJs and showed that the theoretical predictions were consistent well with the experimental results.

The peel stress/strain can be considered as one of the key parameters in the design of adhesively bonded joints. In the present paper, a new strain-based criterion is presented which can be used for failure load prediction of DSJs. The proposed criterion is based on normal (peel) strain along the mid-plane of the adhesive layer. In order to validate the proposed failure criterion, the theoretical results are compared with two series of the experimental data reported in the literature [30, 32] on DSJs. Very good agreement is shown to exist between the experimental and theoretical results.

2. Critical strain-based failure criterion

In this section, a critical distance theory namely the critical normal strain (CNS) criterion is presented in order to predict the failure load values of adhesively bonded double strap joints. The strain normal to the bonding plane is considered as the key parameter in failure load prediction using the CNS criterion. According to this criterion, failure occurs when the normal strain at a specific critical distance, L_c along the adhesive mid-plane attains a critical value, ε_c. In order to calculate the two critical parameters in the CNS criterion i.e. the critical distance and critical strain, at least two double strap joints of different bonding lengths should be tested, and their failure loads are determined. Then, the experimental failure

loads should be applied to 2D linear elastic finite element models of the same test specimens. Afterwards, the normal strain distributions along the adhesive mid-planes of the two simulated joints are plotted versus the normalized bonding length (i.e. the distance from the bonding edge, x divided by the bonding length, L_1). The crossing point of these two graphs would determine the critical normalized distance, L_c and the critical normal strain, ε_c as two constant parameters of the criterion. This procedure is schematically shown in Fig. 2. Now, in order to obtain the failure load for a new DSJ with a different bonding length, a unit external load should be applied to its linear elastic FE model. The ratio of critical normal strain, ε_c to the resultant value of normal strain ($\varepsilon_{\text{unit load}}$) at the specified critical distance, L_c gives the failure load of the joint (i.e. failure load, $P_{CNS} = \varepsilon_c / \varepsilon_{\text{unit load}}$). In the forthcoming sections, first, a series of experimental data reported by Fawzia et al. [30] are described. After that, using finite element modelling the critical parameters L_c and ε_c are extracted for the tested DSJ. Afterwards, failure loads are predicted for some other DSJs tested by Fawzia et al. [30].

3. Experimental results on DSJs

Fawzia et al. [30] conducted a series of experiments on steel/CFRP DSJs to provide detailed understanding of bond characteristics of strengthened DSJs under tension. The results of the experiments performed by Fawzia et al. are named as the results series A in the present paper. They prepared DSJs of different bonding lengths to investigate the bonding length effects on failure in DSJs. Every test sample was made of two steel plates and three CFRP sheets on each side of the joints, as shown in Fig. 1. The adherends were assembled together with Araldate 420 adhesive. The thickness, width and length of steel adherends were t_{st} = 6 mm, B = 50 mm and L_{st} = 400 mm, respectively. Each layer of CFRP had a thickness of 0.18 mm, while the thickness of the adhesive layer was 0.47 mm. Therefore, three layers of CFRP were composed of two adhesive layers to produce a total thickness of 1.48 mm.

In order to provide better mechanical interlocking of substrates (i.e. steel plates), they performed angular grinding of the bonding surfaces followed by acetone washing. The DSJs were cured for 24 hours. In the second step, they have applied uniformly adhesive layer on the steel plate along the bonded joint. After that, the first CFRP laminate was placed up on top of the adhesive layer. For providing DSJs with three layers of CFRP, they have prepared them by considering the mentioned principles above about preparing process of DSJs. Therefore, two layers of CFRP laminates were placed on the first layer of CFRP and the DSJ has been cured for a few days. Consequently, three layers of CFRP have been applied on the other side of the substrates by applying above mentioned preparing method. For the final step, all DSJs have been cured for 7 days at room temperature and then, post curing has been applied at 70° C for one day.

The mechanical properties of these materials are presented in Table 1. In finite element modeling of the adhesive joints, three layers of CFRP and two layers of adhesive between them were considered as one part having an equivalent tensile modulus. The equivalent modulus of this layer was calculated from [31]

$$E_{eq} = \frac{E_{adh} \times t_{adh} + E_{CFRP} \times t_{CFRP}}{t_{adh} + t_{CFRP}}$$

where E_{eq} is the equivalent modulus of CFRP/adhesive layer, and E_{adh} and E_{CFRP} are the tensile modulus of the adhesive layer and CFRP sheets, respectively. The terms t_{adh} and t_{CFRP} represent the total thickness of the adhesive and CFRP layers. The bonding length L_1 was always kept less than L_2 to ensure that the failure occurred on the L_1 side only [30] (see Fig. 1). Details of each test including the dimensions of specimens and the failure loads are listed in Table 2.

4. Finite element analysis

As described in section 2, finite element analyses were performed on two double strap joints with bonding lengths L_1 of 80 mm and 250 mm using ABAQUS software to achieve the normal strain

distribution across the adhesive mid-line in the 2D model of specimens. Due to symmetry, only one half of the adhesive joints was modeled (see Fig. 3). The boundary and loading conditions applied to the finite element models are shown in Fig. 3. Moreover, the adhesive mid-plane and the singularity points of stress/strain in the adhesive layer are illustrated in Fig. 3. The eight-node biquadratic plane strain quadrilateral elements with reduced integration were used for finite element simulation of adhesive joints. A mesh convergence study was also undertaken to ensure that a proper number of elements was used for each finite element analysis. Higher mesh density was used in the adhesive mid-plane to improve the accuracy of the output results. Fig. 4 shows a typical mesh pattern used for the simulated double strap joints. In order to check the possible plastic deformation of the steel substrates, failure loads of the tested joints were applied to finite element models of DSJs with different bonding lengths and negligible plasticity was observed in the substrates. An assumption of linear elastic behavior is appropriate for most of the structural adhesives which behave predominantly in a linear manner until the failure of the joint and is correct for a wide range of configurations [24].

5. Results and discussion

In section 2, the procedure for obtaining the critical normal strain and the critical distance along the adhesive mid-plane layer based on CNS criterion was explained in details. In this section, the results of CNS criterion are compared with the experimental results given in Table 2 to validate the methodology.

5.1. Failure load prediction

Fig. 5 shows the curves of normal strain for the joints series A with two arbitrarily selected bonding lengths L_1 of 80 mm and 250 mm, in terms of the normalized distance along the bonding length. The curves cross each other around a specific point. The values of critical normal strain and critical normalized distance (the two major parameters in the CNS criterion) can be obtained from the crossing point. According to Fig. 5, the CNS constants for the bonding lengths of 80 mm and 250 mm as the

reference joints, are 0.363 for the normalized critical distance and 319με for the critical normal strain. In order to better compare the critical normal strain values, they're presented in micro scale ($\times 10^6$). In some cases, more than one crossing point may exist between the two normal strain curves; then, the crossing point which is farther from the bonding edge should be used to define the critical parameters. This happens when the bonding length is short, and the trend of normal strain distribution is slightly different from longer bonding lengths. This suggestion can be checked by testing more than two samples with different bonding lengths and then obtaining the crossing point of the normal strain distribution for the tested joints. Fig. 6 shows comparison between the estimated failure loads for the remaining joints (L_1 = 150 mm, 200 mm) using the CNS method and the experimental data. More details of each experiment and CNS predictions are presented in Table 2. Good agreement is seen between the CNS predictions and the experimental results. Since acceptable theoretical predictions obtained from CNS criterion were conducted without applying any plasticity properties in the whole of FE analyses, the authors are in believed that a negligible plasticity exist on failure behavior of DSJs.

For further validation, the proposed criterion was used to predict the failure loads in some other double strap adhesive joints which have been reported in a previous experimental study by Fawzia et al. [32] (results series B). Fawzia et al. [32] conducted some experiments on DSJs of width 50 mm and bonding lengths of L_1 = 20, 40, 50, 70 and 80 mm. The DSJs were made from steel plates of 210 mm length and 50 mm width, reinforced on both sides with three layers of CFRP sheets. They used Araldite 420 adhesive for joining the CFRP sheets together and also joining them to the steel plates, and then cured the specimens for 7 days and post cured for one day at 70° C. The mechanical properties and the dimensions of the tested joints are presented in Tables 3 and 4, respectively. A similar method was applied to obtain the normal strain along the bonding length by applying the failure loads to the finite element models. Fig. 7 shows the curves of normal strain along the adhesive bonding length for the series B and bonding lengths L_1 of 20 mm and 80 mm. According to the crossing points in Fig. 7, the constants of CNS criterion for the double strap joint configurations tested by Fawzia et al. [32], are

0.271 for the normalized distance and 359με for the critical normal strain. Using these critical parameters, the failure loads of the remaining joints (L_1 = 40, 50 and 70 mm) were estimated using the CNS criterion. A comparison between the CNS predictions and the experimental results is illustrated in Fig. 8. Again, a very good correlation is seen between the experimental data and CNS estimates for failure loads in the tested DSJs. Fawzia et al. [32] reported that a cohesive failure in adhesive layer was observed in almost all of the tested DSJs.

5.2. Failure load prediction using other joints

As described earlier, the failure loads of DSJs were predicted using two arbitrary selected reference joints. In this section, two different joints are selected as the new reference joints to investigate the sensitivity of the CNS criterion to the choice of reference joints. The normalized critical length, the critical normal strain and finally the CNS failure load predictions for all of the tested DSJs based on the new reference joints are presented in Figs. 9 to 12. It can be observed that the critical parameters are almost independent of the choice of the reference adhesive joints. Moreover, the failure predictions based on two new reference joints are again in good agreement with the experimental results. As mentioned before, it is necessary to test at least two DSJs with different bonding lengths to obtain the CNS constants. However, more experiments with larger numbers of bonding lengths will result in more accurate CNS constants. According to the results presented in this paper, it is deduced that the normal strain is a very appropriate parameter to predict the failure load in the double strap adhesive joints.

5.3. How much does this criterion depend on the element size?

To evaluate the effect of element size on the accuracy of the results determined by the CNS criterion, five different element sizes along the adhesive mid-plane were considered. Table 5 presents the values of normalized critical distance and critical normal strain obtained for the joints series A with L_1 = 80, 250 mm when the element sizes reduced in four steps from 235×235μm to 14.7×14.7μm. It is seen that

the critical characteristics have negligible dependency on the size of elements. Similar results were attained for other adhesive joints in this research.

5.4. The failure mechanisms of steel/CFRP DSJs

The failure mechanisms of steel/CFRP double strap joints can be divided into six categories including failure in adhesive layer (cohesive failure), debonding between CFRP and adhesive layer or between steel plates and adhesive layer (adhesive failure), CFRP rupture and delamination, and steel plates yielding [39]. Fig. 13 illustrates a schematic of these failure mechanisms in CFRP/steel DSJs. In another research, Al-Mosawe et al. [41] studied different types of failure modes in steel/CFRP double strap joints. They investigated the effect of failure modes in stress variations along the bonding length and compared these data with the results presented by Al-Zubaidy et al. [42]. The dominant failure modes in the studied DSJs in this research as reported in references [30, 32] were adhesive failure and steel/adhesive interface debonding. By considering the failure parameters within the adhesive layer, the CNS criterion results in the best failure predictions for the adhesive joints failed in adhesive layer.

Different approaches for failure prediction, such as strain, stress and energy-based criteria have also been suggested in literature (see Ref. [43-49]). Moradi et al. [50] and Hell et al. [26] proposed two stress and energy-based approaches for evaluating the failure in adhesive joints. They proved that both of these criteria are dependent on the element size and have sensitivity for singular points; while as discussed above, the proposed CNS criterion has little sensitivity to element size and singular points. Additionally, some failure prediction methods require consideration of material nonlinear behavior in finite element simulation and also need more material properties to predict the failure loads of the adhesive joints [46, 51].

5.5. Limitations and Advantages of the CNS criterion for DSJs

According to the experimental data, the load-displacement curves of the tested DSJs experienced the linear behavior, leading to final fracture which happened suddenly without any significant plastic deformations in the adhesive layer. In other words the adherents and adhesive experienced only linear elastic conditions. Therefore, it can be expected that the linear elastic fracture mechanics assumption can be utilized for predicting the failure load values of the tested DSJs. In fact, the failure model proposed in the present research (i.e. CNS criterion) can be applied only for the joints experiencing predominantly elastic behavior or little plastic deformations before reaching to the critical failure load.

Some limitations and advantages can be found for the CNS criterion for DSJs. Generally, it is very important to note that the parameter "failure" in CNS failure model for DSJs was utilized only for DSJs experienced adhesive failure or steel/adhesive interface debonding. As can be seen in Tables 2 and 4, the failure load predictions obtained from CNS criterion were in good agreement with the experimental results.

According to CNS criterion, two DSJ should be tested and then their corresponding failure loads applied to their FE analyses to predict the failure loads of DSJs with different bonding lengths, which can be realized as a weak point of this criterion. On the other hand, in some researches dealing with experiments on steel/CFRP DSJs, complicated numerical were applied to the FE analyses. For instance, it can be referred to three researches [16, 32, 33]. According to the mentioned discussions, it can be expressed that if one of the failure model succeeded with high performance in predicting the failure loads values of the tested DSJs does not delivered this message that other failure models could not be utilized and developed. As a consequence, the designers and engineers should always response to this issue that which one of the failure models could be applicable in their own theoretical predictions.

However, in the CNS criterion failure can be easily predicted only by conducting a 2D-linear elastic analysis and consideration of two critical constants. Due to the advantages noted above, one may recommend the use of CNS criterion for predicting the failure load in the steel/CFRP double strap

joints. Although 2D numerical analyses were used in the current research, additional 3D analyses can be performed to check the three-dimensional effects on the strain condition of various bonding lengths. According to the results of the current research, it can be concluded that the critical parameters L_c and ε_c are functions of the material properties of the substrates, adhesive and CFRP sheets. Although, the results presented in this paper were obtained for the steel/CFRP DSJs, the same approach can be examined to estimate the failure load in other metallic alloys and FRP materials.

6. Conclusions

Using the CFRP sheets as an external bonding is an effective approach to overhaul the damaged steel structures. In the present research, a new criterion namely critical normal strain was presented for failure load prediction in the adhesively bonded double strap joints based on normal strain along the adhesive mid-plane. According to this criterion, failure in a double strap joint occurs when the normal strain along the adhesive mid-plane attains a critical value at a specified critical distance. The theoretical predictions of failure loads were compared with experimental data taken from literature. Two sets of experimental results reported for failure loads in steel/CFRP DSJs of different bonding lengths were successfully predicted by means of the CNS criterion. Finally, it was shown that the average accuracy of this criterion was very good, and the strain-based criterion could estimate the experimental failure loads with average discrepancies of about 5 and 5.2 % for series A and B, respectively.

References

[1] Miller TC, Chajes MJ, Mertz DR.: Hastings JN. Strengthening of a steel bridge girder using CFRP plates. J. Bridge Eng. 6, 514-522 (2001)

[2] Bocciarelli M, Colombi P, Fava G, Poggi C.: Prediction of debonding strength of tensile steel/CFRP joints using fracture mechanics and stress based criteria. Eng. Fract. Mech. 76, 299-313 (2009)

[3] Liu H, Xiao Z, Zhao XL, Al-Mahaidi R.: Prediction of fatigue life for CFRP-strengthened steel plates. Thin Walled Struct. 47, 1069-1077 (2009)

[4] Teng JG, Fernando D, Yu T.: Finite element modelling of debonding failures in steel beams flexurally strengthened with CFRP laminates. Eng. Struct. 86, 213-224 (2015)

[5] Kazem H, Guaderrama L, Selim H, Rizkalla S, Kobayashi A.: Strengthening of steel plates subjected to uniaxial compression using small-diameter CFRP strands. Constr. Build. Mater. 111, 223-236 (2016)

[6] Meng F, Li W, Fan H, Zhou Y.: A nonlinear theory for CFRP strengthened aluminum beam. Compos. Struct. 131, 574-577 (2015)

[7] Kashfuddoja M, Ramji M.: Assessment of local strain field in adhesive layer of an unsymmetrically repaired CFRP panel using digital image correlation. Int. J. Adhes. Adhes. 57, 57-69 (2015)

[8] Kashfuddoja M, Ramji M.: Whole-field strain analysis and damage assessment of adhesively bonded patch repair of CFRP laminates using 3D-DIC and FEA. Composites Part B. 53, 46-61 (2013)

[9] Verbruggen S, Aggelis DG, Tysmans T, Wastiels J.: Bending of beams externally reinforced with TRC and CFRP monitored by DIC and AE. Compos. Struct. 112, 113-121 (2014)

[10] Srilakshmi R, Ramji M, Chinthapenta V.: Fatigue crack growth study of CFRP patch repaired Al 2014-T6 panel having an inclined center crack using FEA and DIC. Eng. Fract. Mech. 134, 182-201 (2015)

[11] Ahmad H, Crocombe AD, Smith PA.: Strength prediction in CFRP woven laminate bolted double-lap joints under quasi-static loading using XFEM. Composites Part A. 56, 192-202 (2014)

[12] Ahmad H, Crocombe AD, Smith PA.: Strength prediction in CFRP woven laminate bolted single-lap joints under quasi-static loading using XFEM. Composites Part A. 66, 82-93 (2014)

[13] Ataş A, Soutis C.: Application of cohesive zone elements in damage analysis of composites: Strength prediction of a single-bolted joint in CFRP laminates. Int. J. Non Linear Mech. 66, 96-104 (2014)

[14] Ataş A, Soutis C.: Strength prediction of bolted joints in CFRP composite laminates using cohesive zone elements. Composites Part B. 58, 25-34 (2014)

[15] Campilho RDSG, De Moura MFSF, Domingues JJMS.: Using a cohesive damage model to predict the tensile behaviour of CFRP single-strap repairs. Int. J. Solids Struct. 45, 1497-512 (2008)

[16] Al-Zubaidy H, Al-Mahaidi R, Zhao XL.: Finite element modelling of CFRP/steel double strap joints subjected to dynamic tensile loadings. Compos. Struct. 99, 48-61 (2013)

[17] Hart-Smith LJ.: Adhesive-bonded single-lap joints: Langley Research Center Hampton, VA; (1973)

[18] Groth HL.: Stress singularities and fracture at interface corners in bonded joints. Int. J. Adhes. Adhes. 8, 107-113 (1988).

[19] Tong L.: Strength of adhesively bonded single-lap and lap-shear joints. Int. J. Solids Struct. 35, 2601-2616 (1998)

[20] De Morais AB, Pereira AB, Teixeira JP, Cavaleiro NC.: Strength of epoxy adhesive-bonded stainless-steel joints. Int. J. Adhes. Adhes. 27, 679-686 (2007)

[21] Karachalios EF, Adams RD, da Silva LFM.: Single lap joints loaded in tension with high strength steel adherends. Int. J. Adhes. Adhes. 43, 81-95 (2013)

[22] Khoramishad H, Razavi SMJ.: Metallic fiber-reinforced adhesively bonded joints. Int. J. Adhes. Adhes. 55, 114-122 (2014)

[23] Ayatollahi MR, Nemati Giv A, Razavi SMJ, Khoramishad H.: Mechanical properties of adhesively single lap bonded joints reinforced with multi-walled carbon nanotubes and silica nanoparticles. J. Adhes. (2016)

[24] Ayatollahi MR, Akhavan-Safar A.: Failure load prediction of single lap adhesive joints based on a new linear elastic criterion. Theor. Appl. Fract. Mech. 80, 210-217 (2015)

[25] Chen Z, Adams RD, Da Silva LFM.: Prediction of crack initiation and propagation of adhesive lap joints using an energy failure criterion. Eng. Fract. Mech. 78, 990-1007 (2011)

[26] Hell S, Weißgraeber P, Felger J, Becker W.: A coupled stress and energy criterion for the assessment of crack initiation in single lap joints: a numerical approach. Eng. Fract. Mech. 117, 112-126 (2014)

[27] Chalkley P, Rose F.: Stress analysis of double-strap bonded joints using a variational method. Int. J. Adhes. Adhes. 21, 241-247 (2001)

[28] Barroso A, Mantic V, París F.: Singularity parameter determination in adhesively bonded lap joints for use in failure criteria. Compos. Sci. Technol. 68, 2671-2677 (2008).

[29] Lee HK, Pyo SH, Kim BR.: On joint strengths, peel stresses and failure modes in adhesively bonded double-strap and supported single-lap GFRP joints. Compos. Struct. 87, 44-54 (2009).

[30] Fawzia S, Zhao XL, Al-Mahaidi R.: Bond–slip models for double strap joints strengthened by CFRP. Compos. Struct. 92, 2137-2145 (2010)

[31] Fawzia S, Al-Mahaidi R, Zhao XL.: Experimental and finite element analysis of a double strap joint between steel plates and normal modulus CFRP. Compos. struct. 75, 156-62 (2006)

[32] Fawzia S, Zhao XL, Al-Mahaidi R, Rizkalla S.: Bond characteristics between CFRP and steel plates in double strap joints. Int. Adv. Steel. Const. 1, 17-27 (2005)

[33] Majidi HR, Razavi SMJ, Berto F.: Failure Assessment of Steel/CFRP Double Strap Joints. Metals. 7(7), 255 (2017). (DOI:10.3390/met7070255)

[34] Al-Shawaf A.: Modelling wet lay-up CFRP–steel bond failures at extreme temperatures using stress-based approach. Int. J. Adhes. Adhes. 31, 416-28 (2011)

[35] Nguyen T-C, Bai Y, Zhao XL, Al-Mahaidi R.: Effects of ultraviolet radiation and associated elevated temperature on mechanical performance of steel/CFRP double strap joints. Compos. Struct. 94, 3563-3573 (2012)

[36] Nguyen T-C, Bai Y, Zhao XL, Al-Mahaidi R.: Curing effects on steel/CFRP double strap joints under combined mechanical load, temperature and humidity. Constr. Build. Mater. 40, 899-907 (2013).

[37] Nguyen TC, Bai Y, Zhao XL, Bambach MR, Al-Mahaidi R.: Temperature Effect on Adhesively Bonded CFRP and Steel Double Strap Joints. Advances in FRP Composites in Civil Engineering: Springer. 877-880 (2011)

[38] Nguyen T-C, Bai Y, Zhao XL, Al-Mahaidi R.: Mechanical characterization of steel/CFRP double strap joints at elevated temperatures. Compos. Struct. 93, 1604-1612 (2011)

[39] Zhao XL, Zhang L.: State-of-the-art review on FRP strengthened steel structures. Eng. Struct. 29, 1808-1823 (2007)

[40] Mohee FM, Al-Mayah A, Plumtree A.: Anchors for CFRP plates: State-of-the-art review and future potential. Composites Part B. 90, 432-442 (2016)

[41] Al-Mosawe A, Al-Mahaidi R, Zhao XL.: Effect of CFRP properties, on the bond characteristics between steel and CFRP laminate under quasi-static loading. Constr. Build. Mater. 98, 489-501 (2015)

[42] Al-Zubaidy HA, Zhao X-L, Al-Mahaidi R.: Dynamic bond strength between CFRP sheet and steel. Compos. Struct. 94, 3258-3270 (2012)

[43] Lee SJ, Lee DG.: Development of a failure model for the adhesively bonded tubular single lap joint. J. Adhes. 40, 1-14 (1992)

[44] Gao X-L, Su Y-Y.: An analytical study on peeling of an adhesively bonded joint based on a viscoelastic Bernoulli–Euler beam model. Acta Mech. 226, 3059-3067 (2015)

[45] Voloshko O, Loboda V, Lapusta Y.: Investigation of a crack situated in a thin adhesive layer between two different isotropic materials. Acta Mech. 226, 683-696 (2015)

[46] Harris JA, Adams RA.: Strength prediction of bonded single lap joints by non-linear finite element methods. Int. J. Adhes. Adhes. 4, 65-78 (1984)

[47] Jamali J, Fan Y, Wood J.: The mixed-mode fracture behavior of epoxy by the compact tension shear test. Int. J. Adhes. Adhes. 63, 79-86 (2015)

[48] Jamali J, Mourad AI, Fan Y, Wood J.: Through-thickness fracture behavior of unidirectional glass fibers/epoxy composites under various in-plane loading using the CTS test. Eng. Fract. Mech. 156, 83-95 (2016)

[49] Kim T-U.: The J-integral for single-lap joint using the stress field from the mixed variational principle. Acta Mech. 224, 2611-2622 (2013)

[50] Moradi A, Carrère N, Leguillon D, Martin E, Cognard J-Y.: Strength prediction of bonded assemblies using a coupled criterion under elastic assumptions: Effect of material and geometrical parameters. Int. J. Adhes. Adhes. 47, 73-82 (2013)

[51] Crocombe AD, Adams RD.: An elasto-plastic investigation of the peel test. J. Adhes. 13, 241-267 (1982)

Figure captions

Fig. 1. A schematic of steel/CFRP double strap joint.

Fig. 2. Definition of the local systems of coordinates and experimental determination of ε_c and L_c based on results generated by testing two DSJs with different bonding lengths (joint 1 and joint 2).

Fig. 3. Boundary and loading conditions and the adhesive mid-plane in the double strap adhesive joints.

Fig. 4. A typical finite element mesh for the DSJ configuration.

Fig. 5. Normal strain distribution for joints series A with bonding lengths of L_1 = 80 mm and 250 mm.

Fig. 6. Comparison between the CNS predictions and the experimental failure loads [30] for joints series A (reference bonding lengths: L_1 = 80 mm, 250 mm)

Fig. 7. The curves of normal strain for joints series B with bonding lengths of L_1 = 20 mm and 80 mm.

Fig. 8. Comparison between the CNS predictions and the experimental failure loads [32] for joints series B (reference bonding lengths: L_1 = 20 mm, 80 mm)

Fig. 9. The curves of normal strain for joints series A with bonding lengths of L_1 = 80 mm and 200 mm.

Fig. 10. Comparison between the CNS predictions and the experimental failure loads of joints [30] series A (reference bonding lengths: L_1 = 80 mm, 200 mm)

Fig. 11. The curves of normal strain for joints series B with bonding lengths of L_1 = 20 mm and 70 mm.

Fig. 12. Comparison between the CNS predictions and the experimental failure loads [32] of joints series B (reference bonding lengths: L_1 = 20 mm, 70 mm)

Fig.13. Different types of failure modes of steel/CFRP bonded joint.

Table captions

Table.1 Mechanical properties of materials used for joints series A [30, 31].

Table.2. Dimensions of the adhesive joints and details of experimental and theoretical failure loads for the joints series A.

Table 3. Mechanical properties of specimens in series B [31, 32].

Table 4. The dimensions of adhesive joints and the details of experimental and theoretical failure loads for the joints series B.

Table 5. Mesh sensitivity analysis for the joints series A (L_1 = 80, 250 mm).

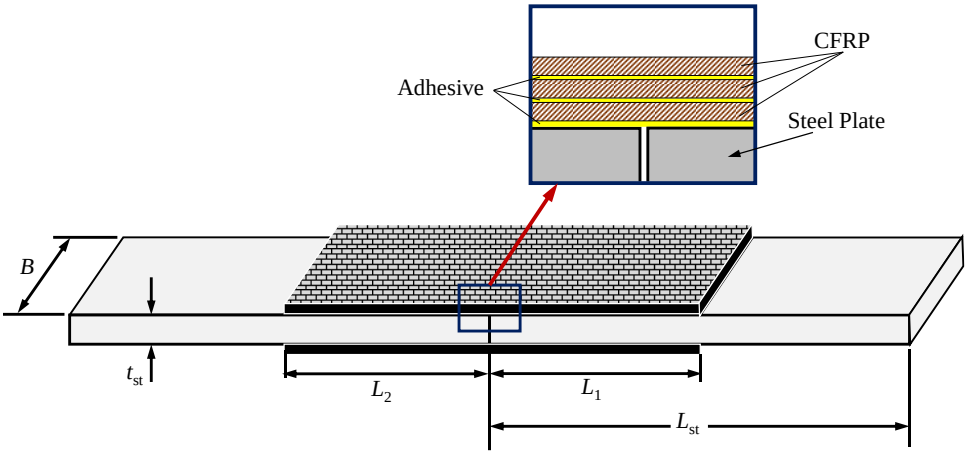

Fig. 1. A schematic of steel/CFRP double strap joint.

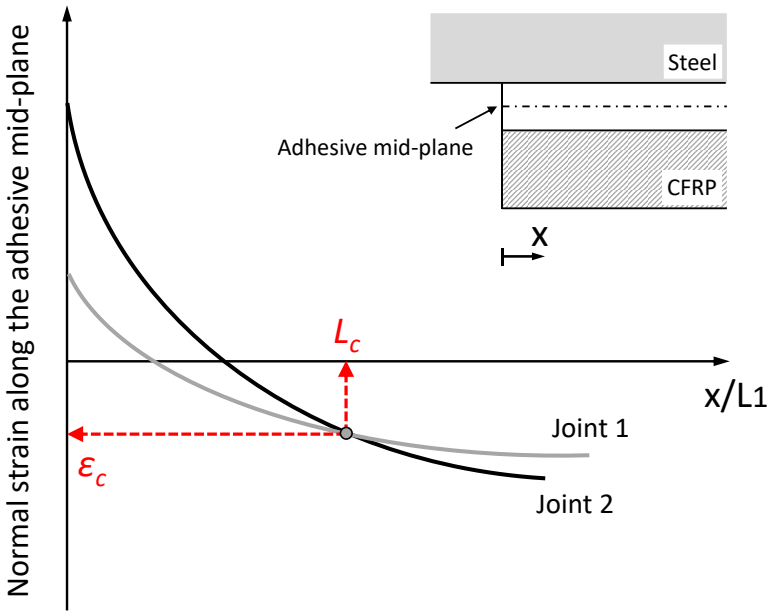

Fig. 2. Definition of the local systems of coordinates and experimental determination of ε_c and L_c based on results generated by testing two DSJs with different bonding lengths (joint 1 and joint 2).

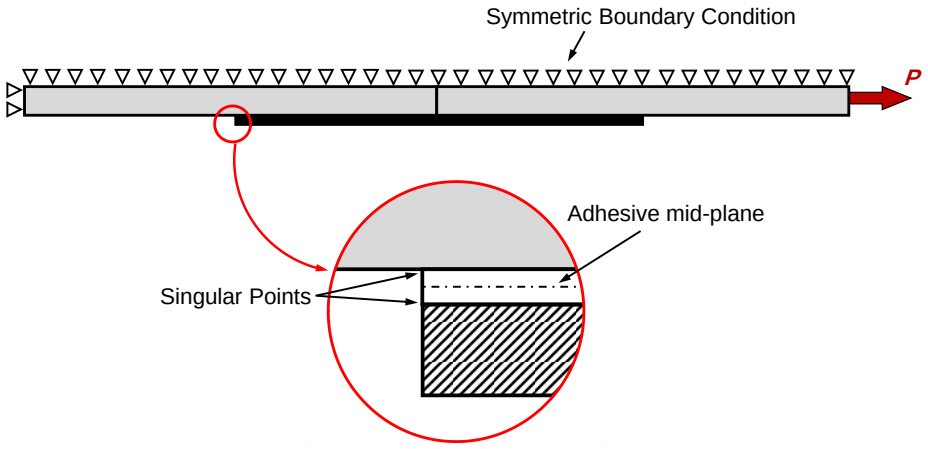

Fig. 3. Boundary and loading conditions and the adhesive mid-plane in the double strap adhesive joints.

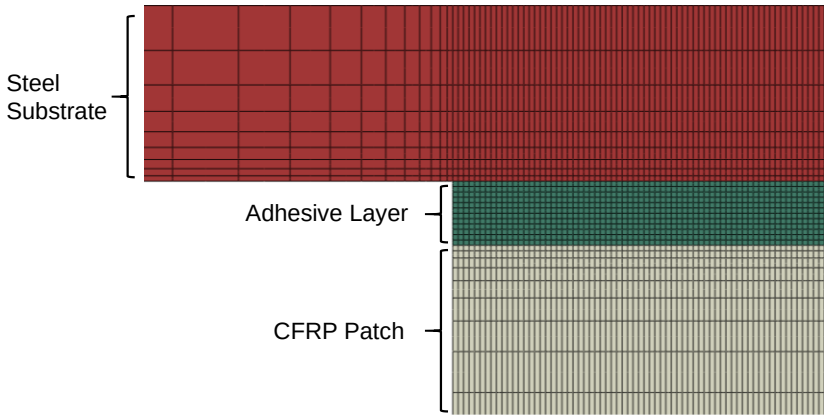

Fig. 4. A typical finite element mesh for the DSJ configuration.

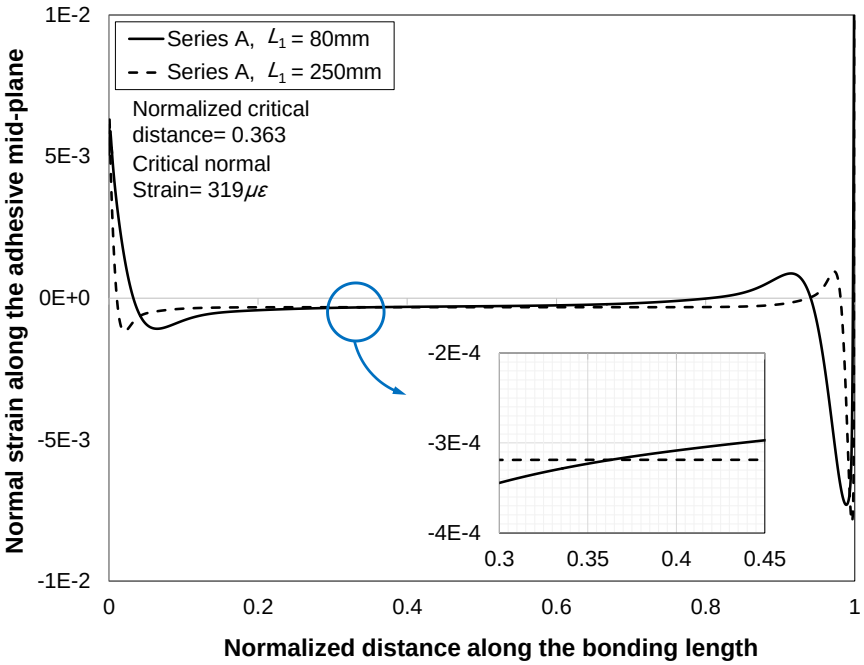

Fig. 5. Normal strain distribution for joints series A with bonding lengths of L_1 = 80 mm and 250 mm.

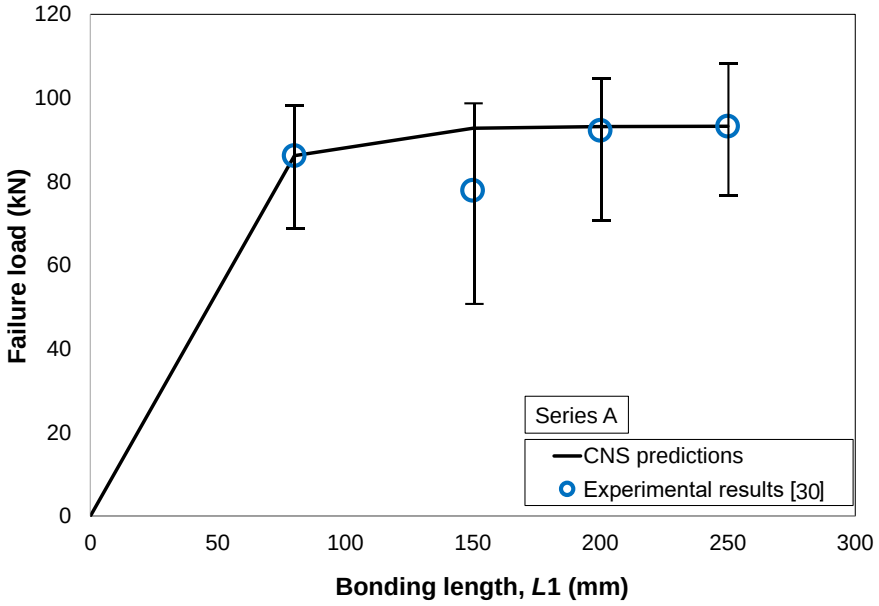

Fig. 6. Comparison between the CNS predictions and the experimental failure loads [30] for joints series A (reference bonding lengths: L_1 = 80 mm, 250 mm)

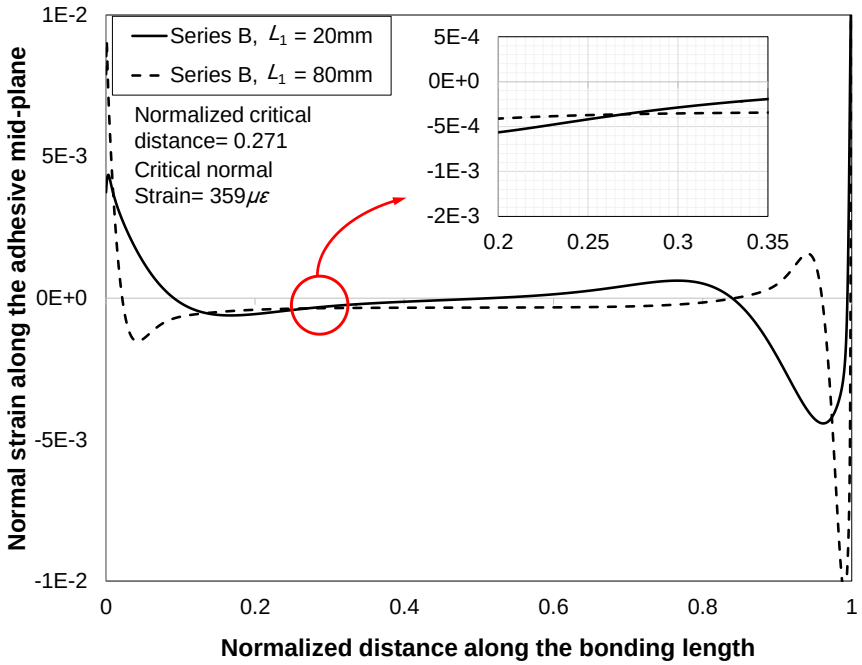

Fig. 7. The curves of normal strain for joints series B with bonding lengths of L_1 = 20 mm and 80 mm.

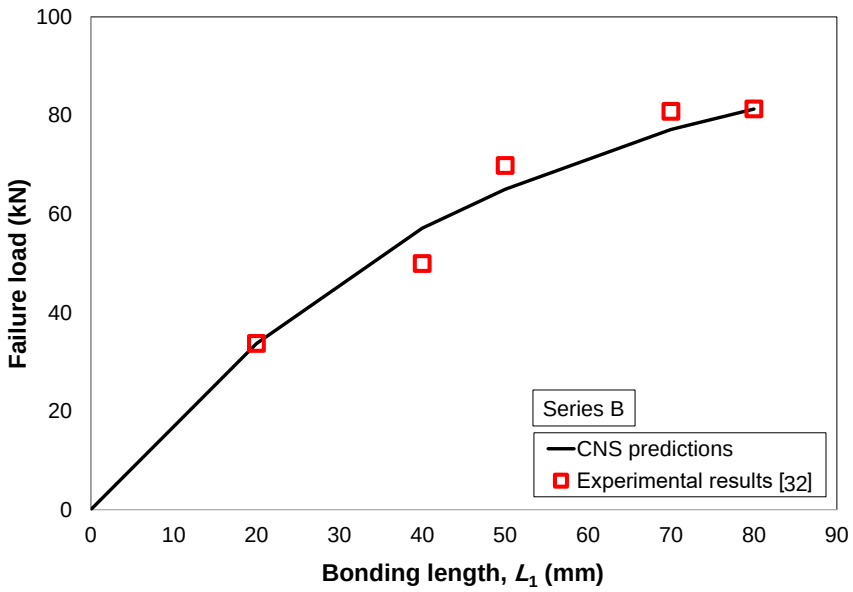

Fig. 8. Comparison between the CNS predictions and the experimental failure loads [32] for joints series B (reference bonding lengths: L_1 = 20 mm, 80 mm)

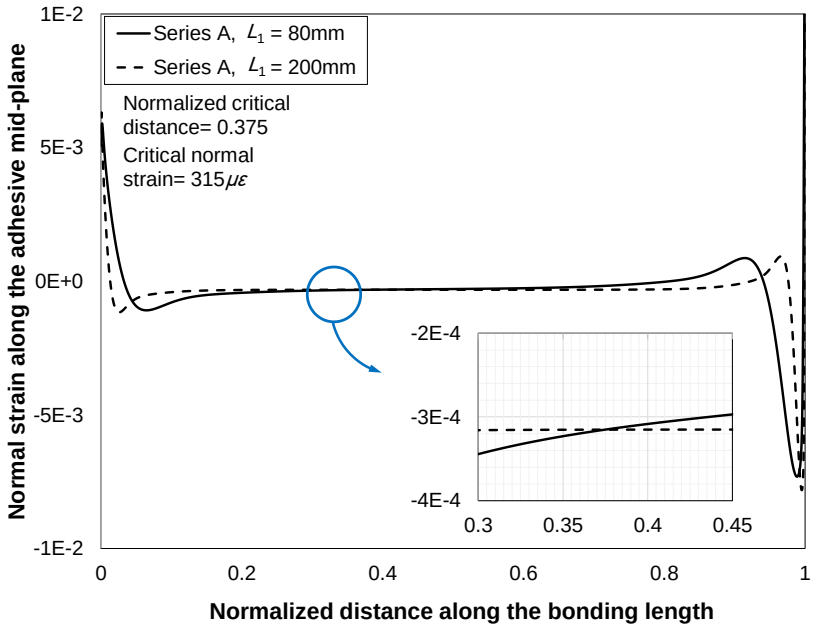

Fig. 9. The curves of normal strain for joints series A with bonding lengths of L_1 = 80 mm and 200 mm.

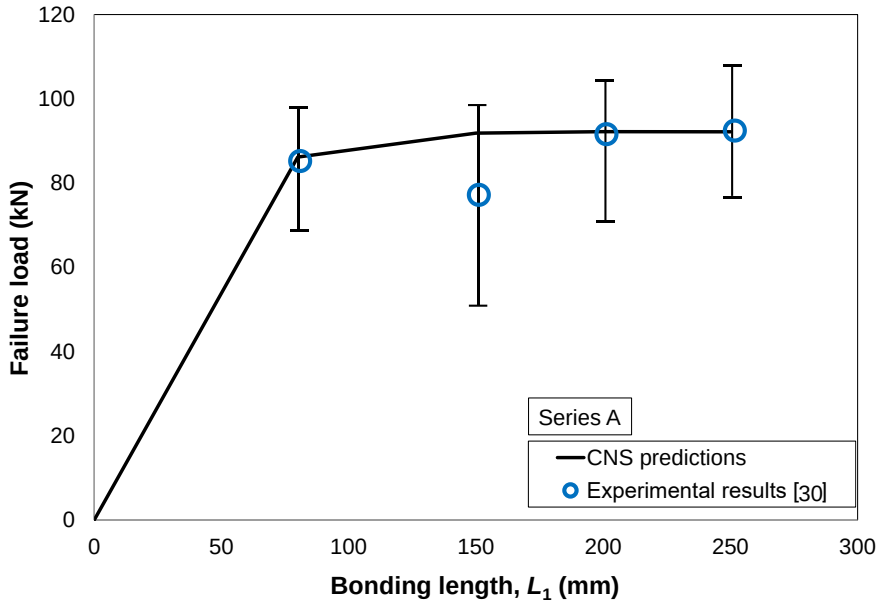

Fig. 10. Comparison between the CNS predictions and the experimental failure loads of joints [30] series A (reference bonding lengths: L_1 = 80 mm, 200 mm)

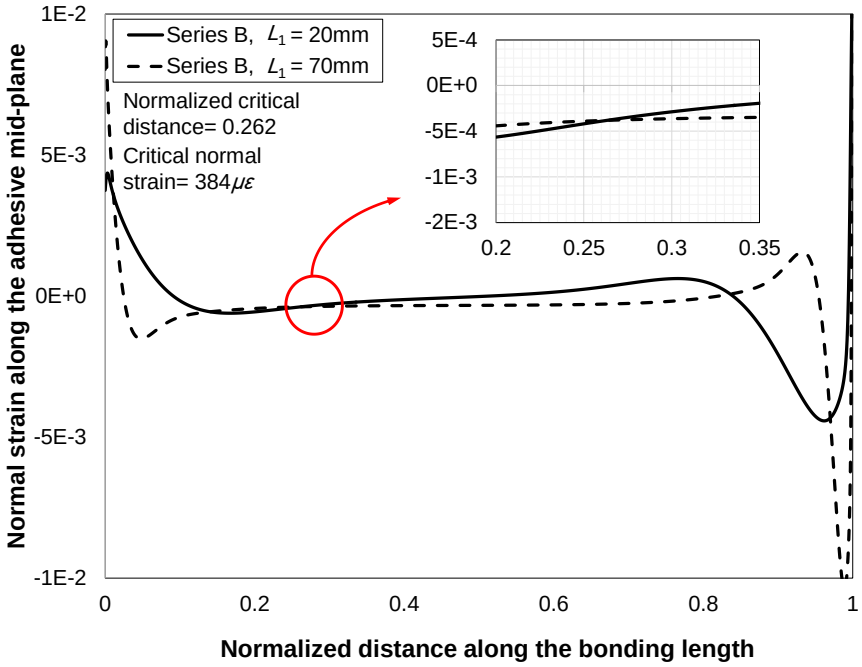

Fig. 11. The curves of normal strain for joints series B with bonding lengths of L_1 = 20 mm and 70 mm.

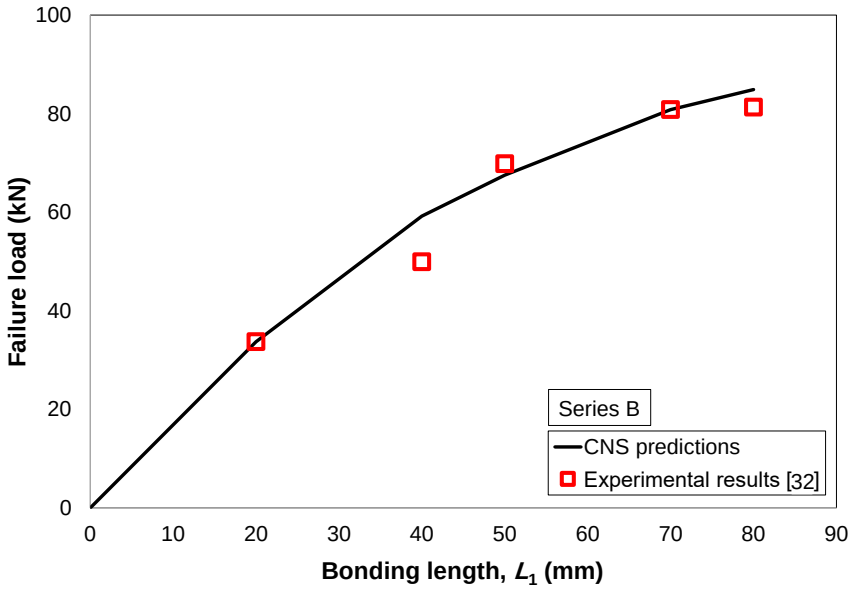

Fig. 12. Comparison between the CNS predictions and the experimental failure loads [32] of joints series B (reference bonding lengths: L_1 = 20 mm, 70 mm)

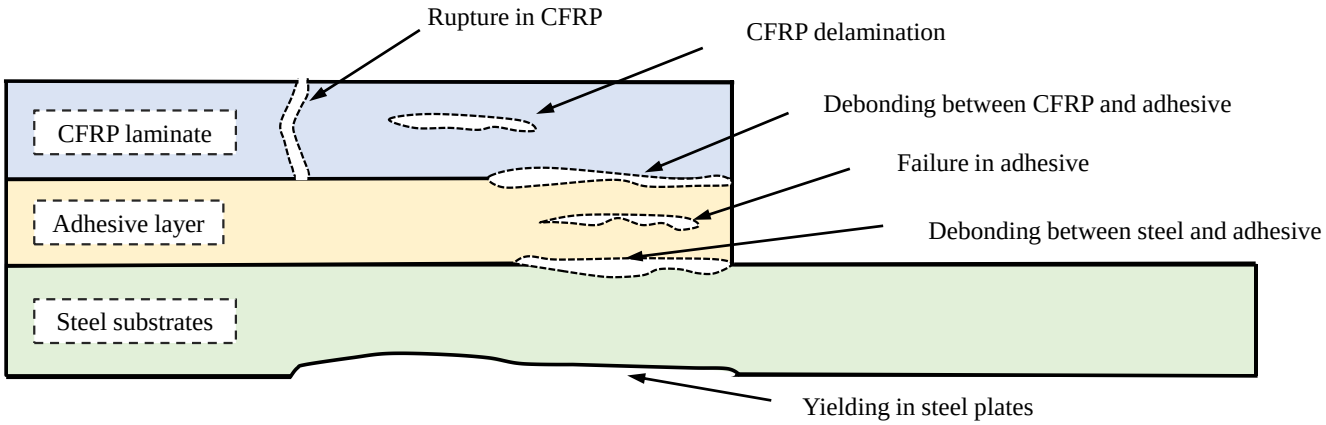

Fig.13. Different types of failure modes of steel/CFRP bonded joint.

Table.1 Mechanical properties of materials used for joints series A [30, 31].

	Steel plates	Adhesive	CFRP sheets
Tensile modulus (GPa)	200	1.9	240
Equivalent tensile modulus (GPa)	----	----	88.7
Poisson's ratio	0.25	0.21	0.28

Table.2. Dimensions of the adhesive joints and details of experimental and theoretical failure loads for the joints series A.

L_1 (mm)	B (mm)	t_{st} (mm)	L_{st} (mm)	t_{adh} (mm)	t_{total} (mm)	$P_{Exp.}$ (kN)	P_{CNS} (kN) [30]	P_{CNS} / $P_{Exp.}$
80	50	6	400	0.47	1.48	98.4 96.9 69.4 80.0 **Avg. = 86.2**	86.2	1
150	50	6	400	0.47	1.48	99.1 70.0 51.4 91.0 **Avg. = 77.9**	92.8	1.19
200	50	6	400	0.47	1.48	92.6 71.6 99.6 105.0 **Avg. = 92.2**	93.1	1.01
250	50	6	400	0.47	1.48	89.6 97.2 77.5 108.6 **Avg. = 93.2**	93.2	1

Table 3. Mechanical properties of specimens in series B [31, 32].

	Steel plates	Adhesive	CFRP sheets
Tensile modulus (GPa)	195	1.9	215
Equivalent tensile modulus (GPa)	-----	-----	117
Poisson's ratio	0.25	0.21	0.28

Table 4. The dimensions of adhesive joints and the details of experimental and theoretical failure loads for the joints series B.

L_1 (mm)	B (mm)	t_{st} (mm)	L_{st} (mm)	t_{adh} (mm)	t_{CFRP} (mm)	$P_{Exp.}$ (kN) [32]	P_{CNS} (kN)	P_{CNS} / $P_{Exp.}$
20	50	5	210	0.224	0.976	33.7	33.7	1
40	50	5	210	0.224	0.976	49.9	57.1	1.14
50	50	5	210	0.224	0.976	69.8	65.0	0.93
70	50	5	210	0.224	0.976	80.8	77.1	0.95
80	50	5	210	0.224	0.976	81.3	81.3	1

Table 5. Mesh sensitivity analysis for the joints series A (L_1 = 80, 250 mm).

Number of elements rows along the adhesive thickness	Element size (mm)	Normalized critical distance	Critical normal strain (με)
2	0.2350	0.367	318.8
4	0.1175	0.364	318.8
8	0.0588	0.364	318.8
16	0.0294	0.363	318.8
32	0.0147	0.363	318.8